Engineering Journal issn: 0125-8281

Article

Automatic Assessment of Seed Germination Percentage

Supawadee Chaivivatrakul

Faculty of Agriculture, Ubon Ratchathani University, Warinchamrap, Ubon Ratchathani 34190, Thailand
E-mail: supawadee.c@ubu.ac.th

Abstract. This research was designed to investigate an automatic seed germination rate for the top of paper germination method. Chili and guinea were adopted to be used in the experiment with a 4-time repetition and 2 sets of the germination group (4-separated plates with 50 seeds per plate, 2 sets per seed type, totally 400 seeds of chili and 400 seeds of quinea). Two detection methods were proposed binary thresholding and maximum likelihood; based on color analysis. An uncontrolled environment image taking was the way to collect image data. The results were compared to a hand-labeling groundtruth. Both methods achieved accuracy rate higher than 93% which was promising to implement this system. The binary thresholding was a lightweight method suitable for a very limited resource software environment system. The maximum likelihood was more complex. The method had more potential than the binary thresholding, it was flexible to the light condition, returned few false alarms per image (less than 3 false alarms per image). Maximum likelihood could be adopted to implement in a proper environment which still could be in a mobile device.

Keywords: Color analysis, object detection, machine vision, seed germination, agriculture.

ENGINEERING JOURNAL Volume 24 Issue 4
Received 4 September 2019
Accepted 15 April 2020
Published 31 July 2020
Online at https://engj.org/
DOI:10.4186/ej.2020.24.4.85

DOI:10.4186/ej.2020.24.4.85

1. Introduction

Seed assessment is an important process to evaluate seed quality for cultivation. The seed germination percentage is one of the outputs from the assessment process, farmers take it to calculate for numbers of seeds per area. Hence, seed companies require to test their products and make labels on them. The seed assessment is the process that is required to be performed by a well-trained or experienced individual. It is also a time-consuming process, especially in the case that there are various kinds of seeds and/or various crops. This would be an issue of human resources. An alternative way for this job is an automatic seed assessment system.

Seed assessment with top of paper method, a method based on ANN (Multilayer perceptron architecture) was proposed to detect seed assessment and obtained 95.44% accuracy [1]. Another researcher group investigated in auto rice seed germination detection based on color, shape and texture analysis. They provided experiments and applications based on their algorithm which yielded more than 90% accuracy rate [2], [3]. Research to detect seed assessment based on image analysis techniques was proposed with high accuracy [4], [5].

Roll of paper method is one of the seed assessment methods. The research adopted a machine learning technique to search for a proper environment: air temperature, and water supply [6]. Machine vision was also adopted to the rolls of paper method in maize seeds [7] and rice seeds [8]. Another seed assessment with wet paper, a low-cost camera monitoring system of the seedling growth support was proposed and experimented [9]. Seed assessment and monitoring with image-based analysis were investigated in many types of imaging such as normal 2D image, NIR image, Hyperspectral image, raman spectroscopy image, infrared thermography image, x-ray image, and etc. [10]–[18]. Most of these studies took data from imaging with some controlled environments, and the systems received very promising results.

Plant, fruit, and leaf detection is a popular object detection task in agriculture. The fruit detection has got a high potential to locate fruits on trees/plants and to classify post-harvested fruits in the grading process as well. Fruit detection could be based on color, shape, and texture analysis [19]–[27]. Numbers of plants or fruits would be the crop yields which was led from the quality of seeds. Properties of plants and leaves could refer to crop health and problem which reflex to crop yield which could be an automatic detection based on image analysis [28], [29].

The object detection could be provided by color, shape, and texture analysis. The color analysis could be performed on various types of color models. The shape analysis could be performed with geometry and non-geometry shape detection. The texture analysis was suitable for the object with texture, the method could be involved with gradient and/or color as well [30][31]. The object detection experiments were investigated in many types of objects, environments, and inputs to the system such as 2D imaging, 3D imaging, stereo imaging, and hyperspectral imaging [32]–[35].

In the approach of supervised learning, we need to perform a training process and a testing process in order to get a predicted model to predict the result. A statistic model that is used to approximate the result is called maximum-likelihood based on Maximization algorithm or EM is a potential method for this kind of task. It calculates posterior values of each group of an object in a training set and makes a model predicting a test set [36], [37].

Nowadays, almost everyone uses smartphones which are known as devices with high-capacity data processing technology. The agriculture family and community also benefit from this advanced technology. The smartphone is a convenient device to take data, provides data processing, and is able to upload data via the Internet accessing. Farmers could use this technology to plan and to monitor the crops and their environments. They could also make their products become standardized to be sold via this channel [38]–[41]. Due to the powerful capacity of the smartphone, convenience, and low-cost device, researchers had investigated smartphones used in the seed testing process to collect and analyze data as well [42], [43].

This research objective was to investigate and to detect seed germination rate by using the top of paper method operated through a machine vision technique. The feasibility testing was performed and was targeted to the mobile devices and flexible environments. The method was tested on two types of seeds: chili and guinea.

2. Materials and Methods

Our method was proposed to detect the germination rate using the top of paper method. A seed germination assessment process was performed by trained-experienced staff members. Chili and guinea seeds were tested. Chili was a representative of the double cotyledon plant seed. Guinea was a representative of the single cotyledon plant seed. We used 2 types of germination plates: rectangle boxes for chili seeds, and petri disks for guinea seeds. The germination plates were kept in a climatic chamber to control light and temperature for the seed germination process. A water supply system was done by hands. Each seed type was germinated into 2 sets, 4 repeats, 50 seeds per plate, so we totally had 8 germination plates per seed type (400 seeds per seed type). The plates were taken to evaluate the germination on day 7^{th} and 14^{th}. On the same day, the images were taken to be used in the automatic detection experiment. A smartphone camera was used to take top view images of the germination plates at a distance of 20 cm. The images were taken under uncontrollable environments. We had provided enough light for human eyes and had taken on a clear view. The image size is 1,280 x 960 pixels. The images were divided into 2 sets; a training set, and a test set. We provided grid search to search for a suited parameter set on the training step. Then, the parameter set was taken into the testing step applying to the separated test set and obtained a

returned germination result as an output. An overview of the system is shown in Fig. 1.

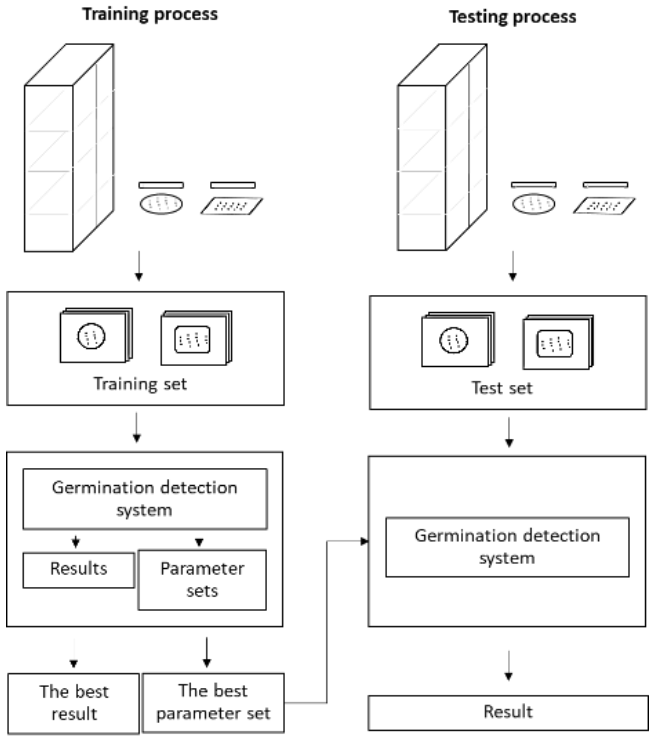

Fig. 1. System overview includes training and testing processes.

In the germination detection system, germination parts of the seeds were detected out of the background. The germination parts were identified by the green parts of the plants that grow out of the seeds. We called the green germination part as foreground and the rest of the image as background. The background included seeds, germination paper, germination plate, and part of a desk.

We experimented with 2 detection methods which were a binary thresholding method and a maximum likelihood method. The methods were implemented in Octave 5.1.0 [44], an open-source software. The detection results were evaluated compared to hand labeling (groundtruth) of the trained-experience staff.

Regarding the detection process, first of all, we removed border pixels of the images, then applied two methods capturing germinated seeds. The binary thresholding method was a method to separate 2 groups of objects based on a dark or a bright color. The maximum likelihood method was more complex than the binary thresholding. We sampled foreground and background pixels from the training set images to make a predicted model for unknown data.

2.1. Border Removal

The border removal removed border pixels of an image which included a border of a box and a desk part that was pasted the seed pates on. The border removal algorithm was provided in Algorithm 1 and the sample result was shown in Fig. 2.

Algorithm 1. BORDER-REMOVAL

Input: I: original image.

Output: I_b: border removal image.

$I_{bw} \leftarrow$ RGB-To-BLACK-AND-WHITE(I)

▸ I_{bw} is a binary image.

$Ig \leftarrow$ RGB-TO-BGRAY(I)

▸ Ig is a grayscale image.

$E \leftarrow$ EDGE(Ig)

▸ E is and edge image.

$I_a \leftarrow$ ADDITION(I_{bw}, E)

▸ I_a is an addition image.

$I_c \leftarrow$ CLOSING(I_a, se_1)

▸ I_c is a closing operation image.

▸ se_1 is a disk-structure element, the radius is 50.

$I_f \leftarrow$ FLOOD-FILL(I_c)

$I_e \leftarrow$ EROSION(I_f, se_2)

▸ I_e is an erosion operation image which is a border pixel image.

▸ se_1 is a disk-structure element, the radius is 15.

r_w=150, g_w=150, b_w=150

$I_b \leftarrow$ GRAY-BORDER-PIXEL(I, I_w)

▸ $(x_w,y_w) \in \{P_w\}_{w \in 1...Nw}$ is a set of border pixels, white pixels in I_e.

▸ $(x_w,y_w) \in \{I_w\}_{w \in 1...Nw}$ is a set of border pixels in the original image I.

$\{I_w\} \subset I$

▸ $(r_w, g_w, b_w) \in \{I_w\}_{w \in 1...Nw}$ is a set r, g, and b value of border pixels in the original image I.

DOI:10.4186/ej.2020.24.4.85

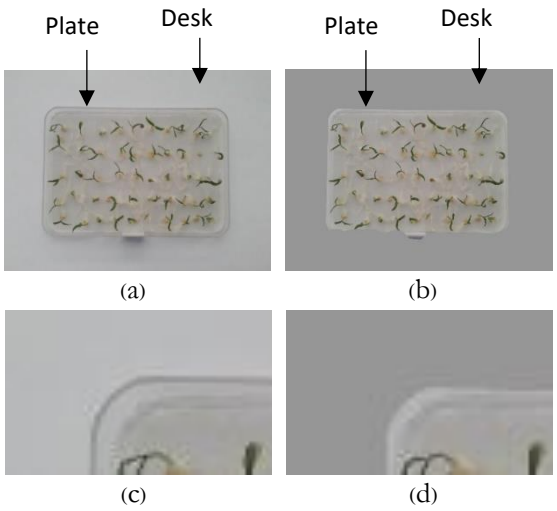

Fig. 2. Border removal. (a) Original image. (b) Border removal image. (c) Zoomed in of the original image. (d) Zoomed in of the border removal image.

2.2. Binary Thresholding

The binary thresholding was performed to separate the foreground which was darker than the background (almost all of the background was brighter than the foreground). Many thresholds were tested to get the proper value to separate the foreground out of the background. Then, the morphological closing operation was applied to combine split parts together. The thresholds were tested between 0.25 to 0.65 and the structured elements of the closing operation were tested in disk-radius 2 to 16. The algorithm was shown in Algorithm 2 and the process with sample image output was shown in Fig. 3.

Algorithm 2. BINARY-THRESHOLDING

Input: I_b: border removal image.

Output: O_b: detected blobs of germinated seeds.

1: $I_{bw} \leftarrow$ RGB-To-BLACK-AND-WHITE(I_b, th)

2: ▸ $th \in \{0.25, 0.30, 0.35, ..., 0.65\}$

3: $I_c \leftarrow$ CLOSING(I_{bw}, se_1)

4: ▸ I_c is a closing operation image.

5: ▸ se_1 is a disk-structure element, radius is in {2, 4, 6, ..., 16}.

6: $O_b \leftarrow$ CONNECTED-COMPONENT(I_c, $\min_i$)

7: ▸ $\min_i$ is minimum pixel numbers, $\min_{chili} = 80$, guinea $\min_{guinea} = 200$

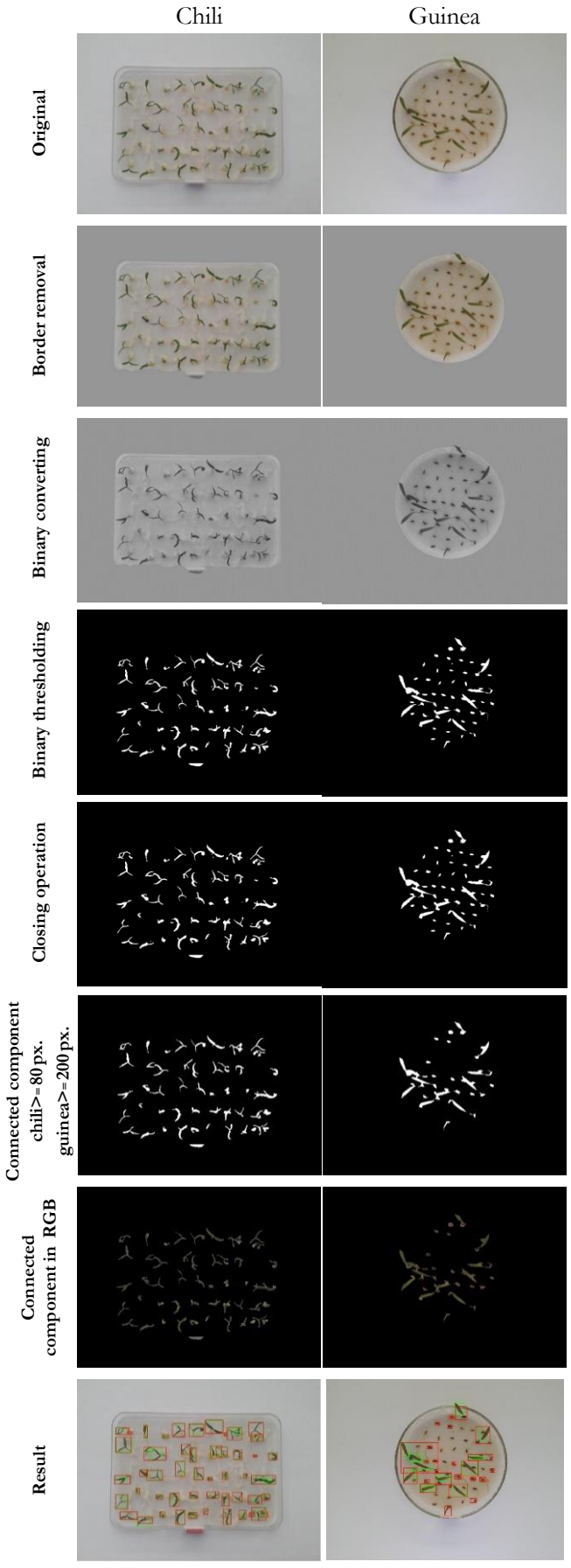

Fig. 3. Binary thresholding, processing steps with sample output images of chili and guinea.

2.3. Maximum Likelihood

Maximum likelihood method was based on the expectation-maximization (EM) algorithm. The training set images were cropped into small pieces of foreground and background manually, as shown in Fig. 4. After that, we provided color analysis for each pixel based on HSV color space. Each pixel value was taken to calculate for posterior values of foreground and background, Eq. (1) [37].

$$P(G|xyz) = \frac{P(xyz|G)P(G)}{P(xyz)} \quad (1)$$

$P(G|xyz)$ is the probability of foreground pixel given point xyz.
$P(xyz|G)$ is the probability of point xyz given foreground pixel.
$P(G)$ is the probability of foreground pixel.
$P(xyz)$ is the probability of point xyz.

(a) (b) (c) (d)

Fig. 4. Maximum likelihood, the training set samples, foreground and background patches. (a) Chili foreground patches. (b) Chili background patches. (c) Guinea foreground patches. (d) Guinea background patches.

We provided the algorithm as in Algorithm 3 which inputs a set of foreground images and a set of background images that manual cropped from the training set (Fig. 4). The sampled output images of each step of Algorithm 3 were represented in Fig. 5.

Algorithm 3. MAXIMUM-LIKELIHOOD

Input: $\{I_{tf}\}$: a set of foreground images, cropped from the training set images
Input: $\{I_{tb}\}$: a set of background images, cropped from the training set images
Input: I_b: border removal image.
Output: O_m: detected blobs of germinated seeds

for each pixel i in $\{I_{tf}\}$
  i' ← RGB-TO-HSV(i)
  (H_{tf},S_{tf},V_{tf}) ← ACCU-COUNT(i'(h,s,v))
end-for
$P_{tf}(H_{tb},S_{tb},V_{tb})$ ← POSTERIOR(H_{tb},S_{tb},V_{tb})
for each pixel i in $\{I_{tb}\}$
  i' ← RGB-TO-HSV(i)
  (H_{tb}, S_{tb}, V_{tb}) ← ACCU-COUNT(i'(h, s, v))
end-for
$P_{tb}(H_{tb}, S_{tb}, V_{tb})$ ← POSTERIOR(H_{tb}, S_{tb}, V_{tb})
I'_b ← RGB-TO-HSV(I_b)
(width, height) ← SIZE(I'_b)
I_{bw} ← BINARY-IMAGE(width, height)
for each pixel i (x_i, y_i) in I'_b
  ▸ i $(x_i, y_i)_{i \in 1...N_i} \in I_{bw}$
  if$(P_{tf}(H_{tb},S_{tb},V_{tb})_i > P_{tb}(H_{tb}, S_{tb}, V_{tb})_i)$
    j (x_i, y_i)=1
    ▸ j $(x_i, y_i)_{i \in 1...N_i} \in I_{bw}$
  other-wise
    j (x_i, y_i)=0
  end
end-for
O_m ← CONNECTED-COMPONENT$(I_{bw}, \min_i)$
  ▸ $\min_i$ is minimum pixel number, $\min_{chili} = 80$, guinea $\min_{guinea} = 200$

In the result evaluation, we considered hit as true positive (TP), miss as false negative (FN), and false alarm as false positive (FP). In some hits cases exist merge and split cases. A merge case occurred when many germinated seeds were merged into one piece. A split case occurred when one germinated seed was divided into many pieces. We provided equations for hits rate (true positive rate), merges rate, splits rate and false alarms per image as in Eq. 2-5. Since we did not consider the true negative (TN) case, we provided the false alarms per image instead of false alarms rate. We counted all false alarms of all images and divided them by the number of images as shown in Eq. 5.

$$Hits\ rate = \frac{Hits}{Hits+Misses} \times 100 \quad (2)$$

$$Merges\ rate = \frac{Merges}{Hits+Misses} \times 100 \quad (3)$$

$$Splits\ rate = \frac{Splits}{Hits+Misses} \times 100 \quad (4)$$

$$False\ alarms\ per\ image = \frac{False\ alarms}{Number\ of\ images} \times 100 \quad (5)$$

3. Experiment and Results

We tested the performance of the 2 methods with the training set and the test set. The criteria employed to get the best parameter set was the result that returned high hits rate, low merges rate, low splits rate, and low false alarms per image. The results were plotted in Figs. 6 - 9.

DOI:10.4186/ej.2020.24.4.85

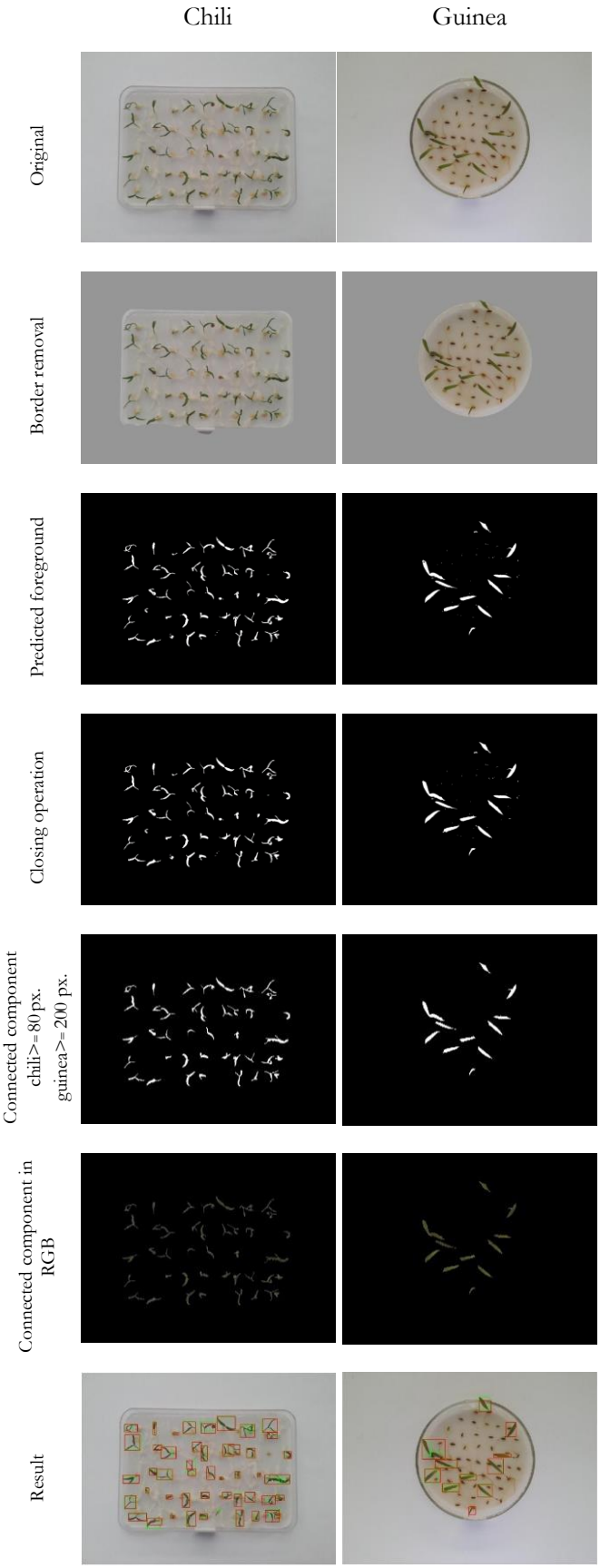

Fig. 5. Maximum likelihood processing steps with sample output images of chili and guinea

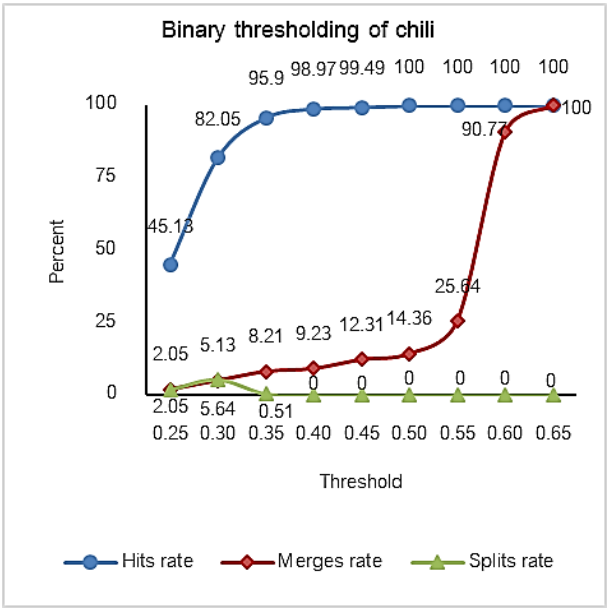

(a)

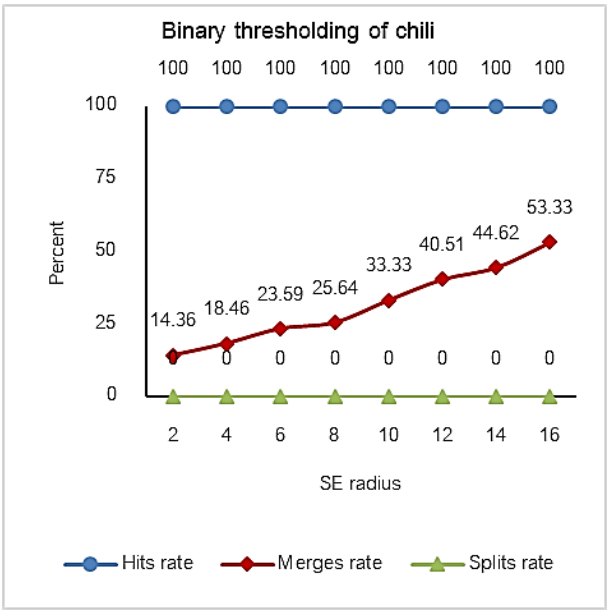

(b)

Fig. 6. Binary thresholding of chili (a) Thresholds 0.25-0.65 (b) Threshold=0.5 and disk structure element radius 2-16

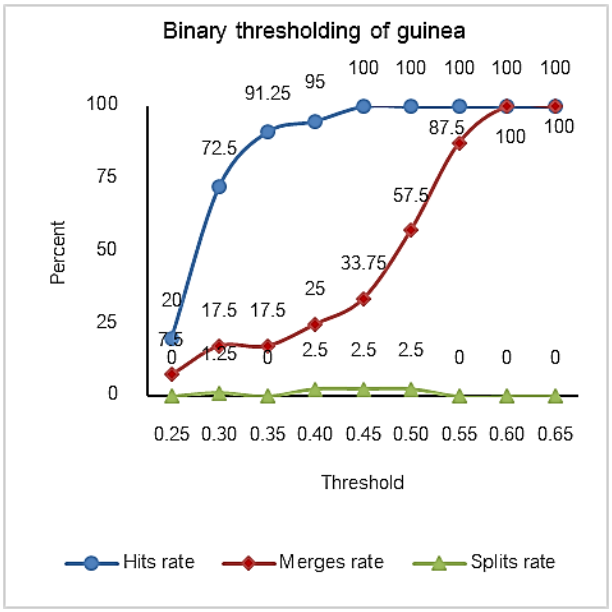

(a)

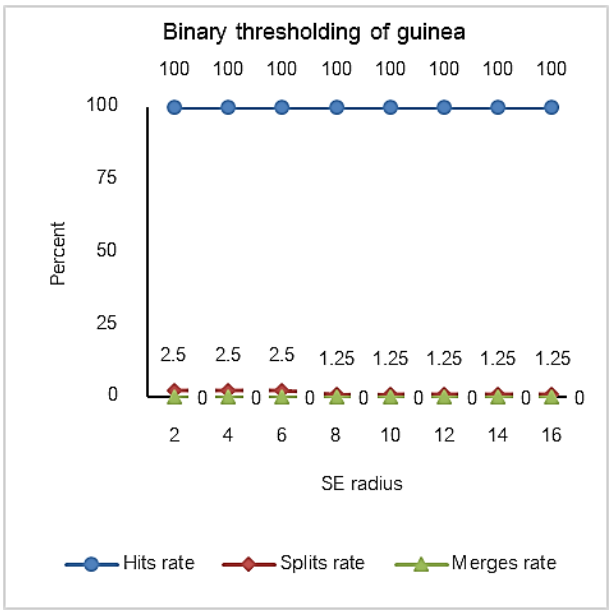

(b)

Fig. 7. Binary thresholding of guinea (a) Thresholds 0.25-0.65 (b) Threshold=0.45 with disk structure element radius 2-16

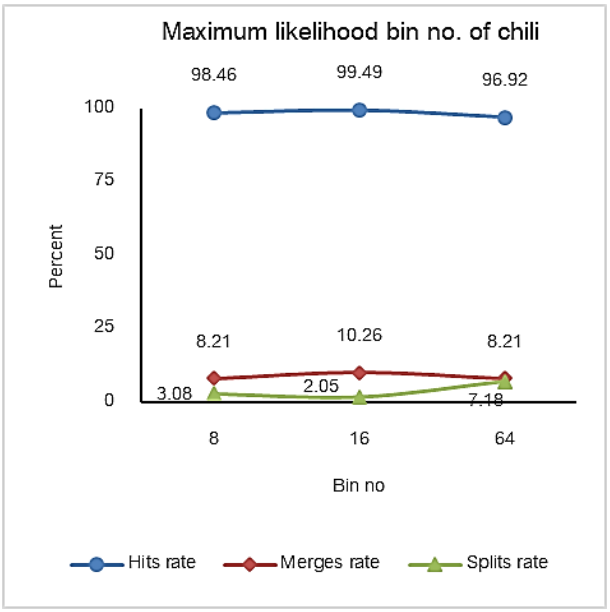

(a)

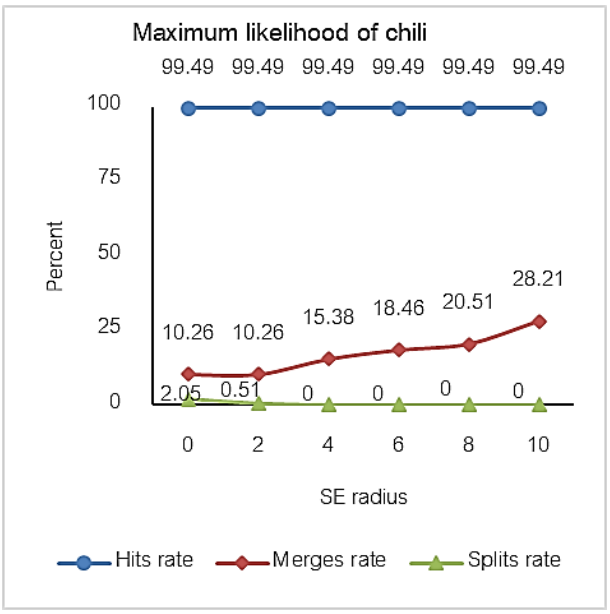

(b)

Fig. 8. Maximum likelihood of chili (a) Bin no = 8, 16, and 64 (b) Bin no = 16, disk structure element radius 0-10

DOI:10.4186/ej.2020.24.4.85

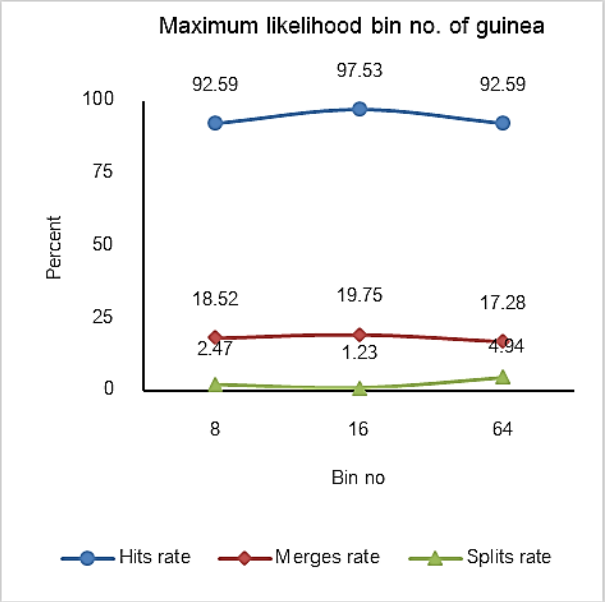

(a)

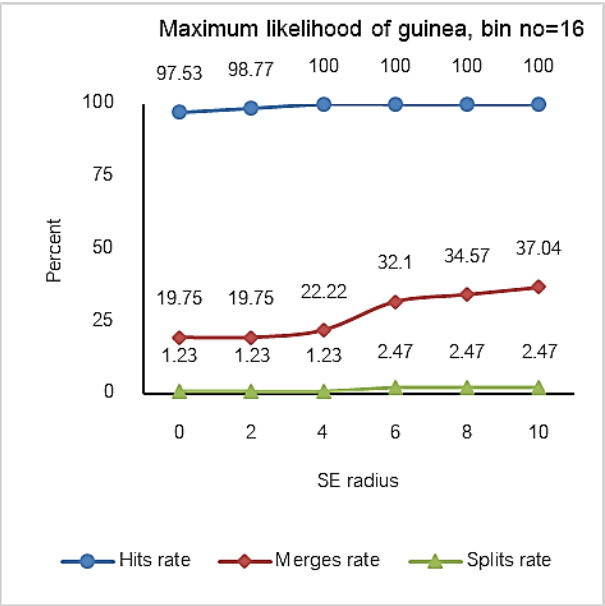

(b)

Fig. 9. Maximum likelihood of guinea (a) Bin no = 8, 16, and 64 (b) Bin no = 16, disk structure element radius 0-10

The binary thresholding, the best parameter set for chili was threshold=0.5, disk structure element radius=2 pixels, and minimum size set to 80 pixels. The result returned hits rate of the training set and the test set of 100% and 100% respectively. The maximum likelihood, the best parameter set for chili was bin no=16, disk structure element radius=2 pixels, and minimum size set to 80 pixels. The result returned hits rate of the training set and the test set of 99.49% and 99.49% respectively.

The best parameter set of guinea was threshold=0.45, disk structure element radius=4 pixels, and minimum size set to 200 pixels. The result returned hits rate of the training set and the test set of 100% and 100% respectively. The maximum likelihood, the best parameter set for the guinea was bin no=16, disk structure element radius=4 pixels, and minimum size set to 200 pixels. The result returned hits rate of the training set and the test set of 100% and 93.65% respectively.

The best parameter sets of the methods were shown in Table 1. The sample evaluation results were shown in Fig. 10 and Fig. 11.

Table 1. The best result of the training set and the result applied to the test set

Seed type Method	Dataset	Hits (%)	Splits (%)	Merges (%)	False alarms per image
Chili Binary thresholding	Training set	100.00	0.00	14.36	16.38
	Test set	100.00	1.54	5.64	15.00
Maximum likelihood	Training set	99.49	0.51	10.26	1.13
	Test set	99.49	2.05	6.67	0.50
Guinea Binary thresholding	Training set	100.00	2.47	35.8	12.75
	Test set	100.00	15.08	52.38	8.88
Maximum likelihood	Training set	100.00	1.23	22.22	0.50
	Test set	93.65	8.73	54.76	2.50

If two (or more) germinated seeds are detected as 1 piece, they will be counted as two (or more) hits and also two (or more) merges (Fig. 12). If two germinated seeds are detected as two pieces separately, they will be counted as two hits and not counted for any merge. Zoomed images of hits with merges are shown in Fig. 12. It is possible that an ungerminated seed is merged with a germinated seed and this will be counted as a hit.

If one germinated seed is detected as 2 (or more) pieces, it will be counted as one hit and also one split. If one germinated seed is detected as one piece, it will be counted as one hit and not counted for any split. Zoomed images of hits with splits are shown in Fig. 13. In the case of a germinated seed detected as 3 pieces and all pieces are big enough to consider as hits, we will count them as a hit and also report this hit as a split. So, splits are a hit (a detected germinated seed) which is split to many pieces.

(a)

(b)

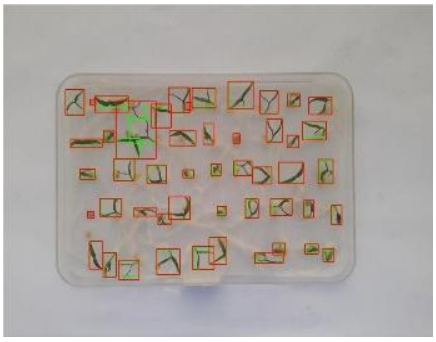

(c)

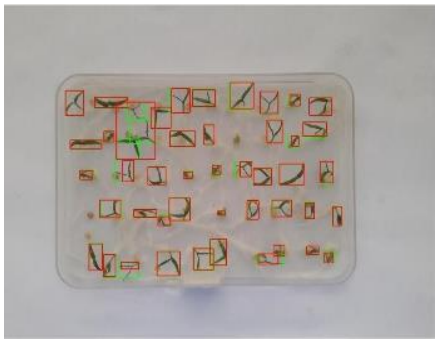

(d)

Fig. 10. Sample image results of chili the binary thresholding and maximum likelihood methods in the same input image; (a-b) Chili training set results, (c-d) Chili test set results; (a) Hits=49, splits=0, merges=6, false alarms=5, misses=0; (b) Hits=48, splits=1, merges=4, false alarms=0, misses=1; (c) Hits=49, splits=0, merges=4, false alarms=1, misses=0; (d) Hits=48, splits=0, merges=0, false alarms=2, misses=1.

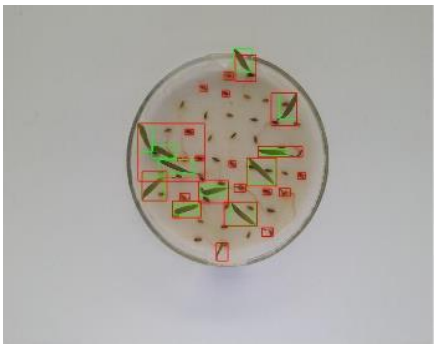

(a)

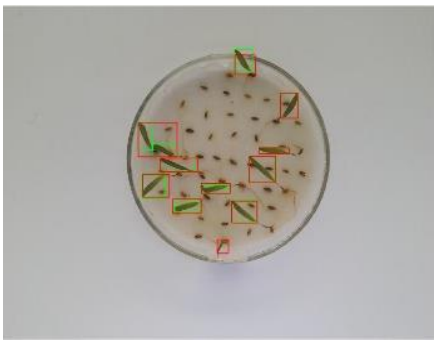

(b)

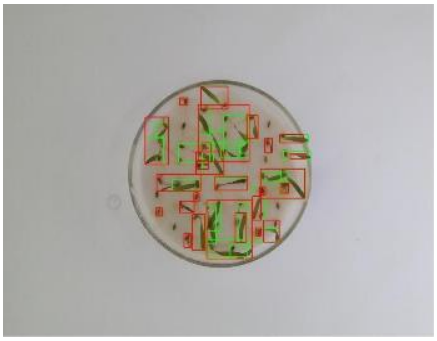

(c)

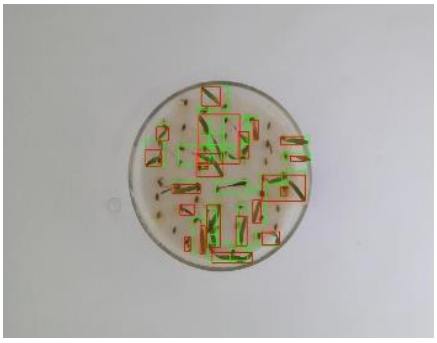

(d)

Fig. 11. Sample image results of guinea with the binary thresholding and maximum likelihood methods in the same input image; (a-b) Guinea training set results, (c-d) Guinea test set results; (a) Hits=11, splits=0, merges=3, false alarms=14, misses=0; (b) Hits=11, splits=0, merges=2, false alarms=1, misses=0; (c) Hits=25, splits=3, merges=15, false alarms=8, misses=0; (d) Hits=24, splits=0, merges=13, false alarms=4, misses=1.

DOI:10.4186/ej.2020.24.4.85

(a) (b)

Fig. 12. Merges, sample zoomed images of hits with merges (a) Chili sample of hits=2, and merges=2 (b) Guinea sample of hits=2, and merges=2.

(a) (b)

Fig. 13. Splits, sample zoomed images of hits with splits (a) Chili sample of hits=1, and splits=1 (b) Guinea sample of hits=1, and splits=1.

Considering running time, the binary thresholding obtained 22.73 seconds per image. This method did not require extra training process. Running time of the maximum likelihood method was 104.03 seconds per image. This method needed an extra training process runs once to get a predicted model of each pixel. The training process of maximum likelihood obtained 0.29 seconds of running time. Table 2 showed running time of the methods.

Table 2. Running time of binary thresholding and maximum likelihood.

Method	Training process, running time once (seconds)	Running time per image (seconds)
Binary thresholding	-	22.73
Maximum likelihood	0.29	104.03

4. Discussion and Conclusion

We proposed two methods to detect seed germination rate automatically. Binary thresholding and maximum likelihood were proposed, implemented, and experimented. The binary thresholding and the maximum likelihood, both methods returned hits rate more than 93% for the training set and the test set. The number of merges and splits cases did not distinguish the difference between these two methods. In the best parameter set result, almost all of the merges cases occurred when the germinated seeds were actually connected. The splits cases mostly occurred in the thin and bright part of the germinated seeds. Many view image analyses could help in merges and splits cases.

The binary thresholding results returned hits rate of 100%; however, the false alarms per image was much higher than the maximum likelihood. Moreover, the maximum likelihood was more tolerated to the darker object than the binary thresholding. Therefore, the maximum likelihood was a better choice to achieve high hits and low false alarms.

To gain higher accuracy in the maximum likelihood, we required more training data set to cover all colors of the foreground and the background to train for a better model. The binary thresholding got a good running time and it was a simple algorithm. Therefore, it was suitable for a very limited resource system. However, the binary thresholding was sensitive to light; therefore, there was a high requirement to take these factors into consideration properly before implementation. On the other hand, maximum likelihood became a more complex algorithm and it was more flexible to the light condition with higher running time. Regarding implementation of a C/C++, or the Java environment, it would support in term of running time. This method would be appropriate to adopt this kind of system.

Octave is open source software and it is a good tool to test the methods with the nice graphic user interface. The Octave has a desktop computer version and also a mobile version that can be switched or used together with the same source code of the other device versions. However, resource management have limitations and it take a high running time. If we implement in a better environment management, a better running time we will be received.

In the case of another set of data with different sizes, we need to provide a new training process to tune the parameters. It would be better to adjust the size of the seed to be related to sizes of the images instead of the fixed size setting. The smaller size/resolution of images will take less running time and will possibly return less accurate result than the larger one. In the case of different seed type which is a difference in size, color, and/or shape need to be started over the training process. Moreover, the number of data set will affect the reliability of the result. The bigger data set, the more reliability of the results will be received.

Specialized equipment and a smartphone/a mobile device benefit the users in many different ways. The specialized equipment that all environments are already set. There is no need for the users to set up anything; however, they need to spend their budget and they also need to carry on this extra device. On the other hand, the smartphone devices are convenient and most people carry them all the time. These devices have compact sizes and they are powerful by sensor systems and Internet connection. To get benefit of the smartphones, we need to provide some settings which are similar to the ones as in this experiment. Thus, smartphone users will have more benefits through this way.

In the case of not controlling the light, posture, and distance, we had provided enough light for human eyes, got top view image, and distance between the camera and the plate was about 20 cm. We received benefits from hand-held-smartphone camera users. Our result was very promising in the dataset. Thus, a smartphone application for this automatic germination percentage could be developed and implemented. Furthermore, with the smartphone, it was very convenient for cloud computing.

Regarding further research studies, we have planned to implement certain methods with a bigger data set, different and various types of seeds. Additionally, a mobile technology application would be incorporated as another task system.

Acknowledgment

We would like to thank for research funding support from the Faculty of Agriculture, Ubon Ratchathani University. Thank you for our plant scientists and agriculture community for their effort and support.

References

[1] U. Škrubej, Č. Rozman, and D. Stajnko, "Assessment of germination rate of the tomato seeds using image processing and machine learning," *Eur. J. Hortic. Sci.*, vol. 80, no. 2, pp. 68–75, 2015.

[2] B. Lurstwut and C. Pornpanomchai, "Rice Seed Germination Analysis," *Int. J. Comput. Appl. Technol. Res.*, vol. 5, no. 4, pp. 176–182, 2016.

[3] B. Lurstwut and C. Pornpanomchai, "Image analysis based on color, shape and texture for rice seed (Oryza sativa L.) germination evaluation," *Agric. Nat. Resour.*, vol. 51, no. 5, pp. 383–389, 2017.

[4] P. P. Belsare and S. K. Shah, "Evaluation of seedling growth rate using image processing," in *IEEE International Conference on Computational Intelligence and Computing Research 2013*, 2013, pp. 1–4.

[5] J. H. Tong, J. B. Li, and H. Y. Jiang, "Machine vision techniques for the evaluation of seedling quality based on leaf area," *Biosyst. Eng.*, vol. 115, no. 3, pp. 369–379, 2013.

[6] A. Nikitin, I. Fastovets, D. Shadrin, M. Pukalchik, and I. Oseledets, "Bayesian optimization for seed germination," *Plant Methods*, vol. 15, no. 1, p. 43, 2019.

[7] D. O. C. Castan, F. G. Gomes-Junior, and J. Marcos-Filho, "Vigor-S, a new system for evaluating the physiological potential of maize seeds," *Sci. Agric.*, vol. 75, pp. 167–172, 2018.

[8] T. T. Nguyen, V. Hoang, T. Le, T. Tran, and H. Vu, "A vision based method for automatic evaluation of germination rate of rice seeds," in *2018 1st International Conference on Multimedia Analysis and Pattern Recognition (MAPR)*, 2018, pp. 1–6.

[9] P. Rasti, D. Demilly, L. Benoit, E. Belin, S. Ducournau, F. Chapeau-Blondeau, and D. Rousseau, "Low-cost vision machine for high-throughput automated monitoring of heterotrophic seedling growth on wet paper support," in *The 29th British Machine Vision Conference (BMVC)*, September 2018, p. 323.

[10] E. Belin, C. Douarre, N. Gillard, F. Franconi, J. Rojas-Varela, F. Chapeau-Blondeau, D. Demilly, J. Adrien, E. Maire, and D. Rousseau, "Evaluation of 3D/2D imaging and image processing techniques for the monitoring of seed imbibition," *J. Imaging*, vol. 4, no. 7, 2018.

[11] Y. Xia, Y. Xu, J. Li, C. Zhang, and S. Fan, "Recent advances in emerging techniques for non-destructive detection of seed viability: A review," *Artif. Intell. Agric.*, vol. 1, pp. 35–47, 2019.

[12] N. D. Miller, S. C. Stelpflug, S. M. Kaeppler, and E. P. Spalding, "A machine vision platform for measuring imbibition of maize kernels: Quantification of genetic effects and correlations with germination," *Plant Methods*, vol. 14, no. 1, p. 115, 2018.

[13] D. Awty-Carroll, J. Clifton-Brown, and P. Robson, "Using k-NN to analyse images of diverse germination phenotypes and detect single seed germination in Miscanthus sinensis," *Plant Methods*, vol. 14, no. 1, p. 5, 2018.

[14] Z. Li, Y. Liu, and R. Liu, "Integrating Multiple-capsule Traits Quantitative Evaluation of Seed Maturity by 3D Phenotypic Platform in Nicotiana tabacum," *HortScience*, vol. 54, no. 6, pp. 993–997, 2019.

[15] K. Tu, L. Li, L. Yang, J. Wang, and Q. Sun, "Selection for high quality pepper seeds by machine vision and classifiers," *J. Integr. Agric.*, vol. 17, no. 9, pp. 1999–2006, 2018.

[16] S. Mahajan, S. K. Mittal, and A. Das, "Machine vision based alternative testing approach for physical purity, viability and vigour testing of soybean seeds (Glycine max)," *J. Food Sci. Technol.*, vol. 55, no. 10, pp. 3949–3959, 2018.

[17] G. ElMasry, N. Mandour, S. Al-Rejaie, E. Belin, and D. Rousseau, "Recent applications of multispectral imaging in seed phenotyping and quality monitoring—An overview," *Sensors*, vol. 19, no. 5, 2019.

[18] G. ElMasry, N. Mandour, M.H. Wagner, D. Demilly, J. Verdier, E. Belin, and D. Rousseau, "Utilization of computer vision and multispectral imaging techniques for classification of cowpea (Vigna unguiculata) seeds," *Plant Methods*, vol. 15, no. 1, p. 24, 2019.

[19] G. Lin, Y. Tang, X. Zou, J. Xiong, and Y. Fang, "Color-, depth-, and shape-based 3D fruit detection," *Precis. Agric.*, 2019.

[20] H. Kuang, C. Liu, L. L. H. Chan, and H. Yan, "Multi-class fruit detection based on image region selection and improved object proposals," *Neurocomputing*, vol. 283, pp. 241–255, 2018.

[21] S. Chaivivatrakul and M. N. Dailey, "Texture-based fruit detection," *Precis. Agric.*, vol. 15, no. 6, pp. 662–683, 2014.

[22] H. Gan, W. S. Lee, V. Alchanatis, R. Ehsani, and J. K. Schueller, "Immature green citrus fruit detection using color and thermal images," *Comput. Electron. Agric.*, vol. 152, pp. 117–125, 2018.

[23] A. Siedliska, P. Baranowski, M. Zubik, W. Mazurek, and B. Sosnowska, "Detection of fungal infections in strawberry fruit by VNIR/SWIR hyperspectral imaging," *Postharvest Biol. Technol.*, vol. 139, pp. 115–126, 2018.

[24] C. Wang, W. S. Lee, X. Zou, D. Choi, H. Gan, and J. Diamond, "Detection and counting of immature green citrus fruit based on the Local Binary Patterns (LBP) feature using illumination-normalized images," *Precis. Agric.*, vol. 19, no. 6, pp. 1062–1083, 2018.

[25] M. Woźniak and D. Połap, "Adaptive neuro-heuristic hybrid model for fruit peel defects detection," *Neural Networks*, vol. 98, pp. 16–33, 2018.

[26] J. J. Zhuang, S. M. Luo, C. J. Hou, Y. Tang, Y. He, and X. Y. Xue, "Detection of orchard citrus fruits using a monocular machine vision-based method for automatic fruit picking applications," *Comput. Electron. Agric.*, vol. 152, pp. 64–73, 2018.

[27] A. Koirala, K. B. Walsh, Z. Wang, and C. McCarthy, "Deep learning for real-time fruit detection and orchard fruit load estimation: Benchmarking of `MangoYOLO'," *Precis. Agric.*, 2019.

[28] C. A. Pulido Rojas, L. E. Solaque Guzman, and N. F. Velasco Toledo, "A comparative analysis of weed images classification approaches in vegetables crops," *Eng. J.*, vol. 21, no. 2, pp. 81–98, 2017.

[29] S. Thaiparnit and M. Ketcham, "A prediction algorithm for paddy leaf chlorophyll using colour model incorporate multiple linear regression," *Eng. J.*, vol. 21, no. 3, pp. 269–280, 2017.

[30] R. Szeliski, *Computer Vision: Algorithms and Applications*, 1st ed. Berlin, Heidelberg: Springer-Verlag, 2010.

[31] R. C. González and R. E. Woods, *Digital Image Processing*, 4th ed. Pearson Education, 2018.

[32] B. Gecer, G. Azzopardi, and N. Petkov, "Color-blob-based COSFIRE filters for object recognition," *Image Vis. Comput.*, vol. 57, pp. 165–174, 2017.

[33] R. Chen, T. Chu, J. A. Landivar, C. Yang, and M. M. Maeda, "Monitoring cotton (Gossypium hirsutum L.) germination using ultrahigh-resolution UAS images," *Precis. Agric.*, vol. 19, no. 1, pp. 161–177, 2018.

[34] X. Chen, K. Kundu, Y. Zhu, H. Ma, S. Fidler, and R. Urtasun, "3D object proposals using stereo imagery for accurate object class detection," *IEEE Trans. Pattern Anal. Mach. Intell.*, vol. 40, no. 5, pp. 1259–1272, 2018.

[35] T. Zhang, W. Wei, B. Zhao, R. Wang, M. Li, L. Yang, J. Wang, and Q. Sun, "A reliable methodology for determining seed viability by using hyperspectral data from two sides of wheat seeds," *Sensors (Switzerland)*, vol. 18, no. 3, 2018.

[36] C. Wang and D. J. Hill, *Deterministic Learning Theory for Identification, Recognition, and Control*. CRC Press, 2009.

[37] K. P. Murphy, *Machine Learning: A Probabilistic Perspective*. MIT Press, 2012.

[38] K. Dehnen-Schmutz, G. L. Foster, L. Owen, and S. Persello, "Exploring the role of smartphone technology for citizen science in agriculture," *Agron. Sustain. Dev.*, vol. 36, no. 2, pp. 1–9, 2016.

[39] W. Ma, R. Q. Grafton, and A. Renwick, "Smartphone use and income growth in rural China: Empirical results and policy implications," *Electron. Commer. Res.*, 2018.

[40] S. Cubero, F. Albert, J. M. Prats-Moltalbán, D. G. Fernández-Pacheco, J. Blasco, and N. Aleixos, "Application for the estimation of the standard citrus colour index (CCI) using image processing in mobile devices," *Biosyst. Eng.*, vol. 167, pp. 63–74, 2018.

[41] V. Bonke, W. Fecke, M. Michels, and O. Musshoff, "Willingness to pay for smartphone apps facilitating sustainable crop protection," *Agron. Sustain. Dev.*, vol. 38, no. 5, 2018.

[42] M. D. Catalano, F. P. Rivera, and R. A. Braga, "Viability of biospeckle laser in mobile devices," *Optik (Stuttg).*, vol. 183, pp. 897–905, 2019.

[43] M. Zhihong, M. Yuhan, G. Liang, and L. Chengliang, "Smartphone-based visual measurement and portable instrumentation for crop seed phenotyping," *IFAC-PapersOnLine*, vol. 49, no. 16, pp. 259–264, 2016.

[44] J. W. Eaton, D. Bateman, S. Hauberg, and R. Wehbring, *GNU Octave Version 5.1.0 Manual: A High-Level Interactive Language for Numerical Computations*. 2019.

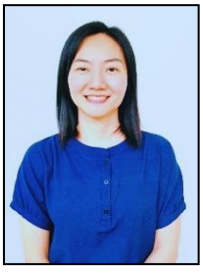

Supawadee Chaivivatrakul received the B.S. and M.S. degrees in computer science from Chiang Mai University, Chiang Mai, Thailand, in 1999 and 2003 respectively and the Ph.D. degree in computer science from Asian Institute of Technology, Bangkok, Thailand in 2014. She was a visiting scholar in Agriculture and Biosystems Engineering, Iowa State University, IA, USA in 2010.

From 2005 she has been a lecturer in Information Technology for Agriculture and Rural Development program, Agriculture Faculty, Ubon Ratchathani University. She has got more than 10 publications in national and international publisher.